Multi-decadal atoll-island dynamics in the Indian Ocean Chagos Archipelago

Mingyue Wu [a], Virginie K.E. Duvat [b], Sam J. Purkis [a,c,*]

[a] CSL – Center for Carbonate Research, Department of Marine Geosciences, Rosenstiel School of Marine and Atmospheric Science, University of Miami, Miami, FL 33149, USA
[b] UMR LIENSs 7266, La Rochelle Université-CNRS, Bâtiment ILE, 2 rue Olympe de Gouges, 17000 La Rochelle, France
[c] Khaled bin Sultan Living Oceans Foundation, 821 Chesapeake Avenue #3568, Annapolis, MD 21403, USA

A B S T R A C T

This study calls upon recently discovered aerial photographs for two atolls in the Indian Ocean Chagos Archipelago. Pairing these vintage data with modern satellite imagery allows the coastline dynamics of a suite of islands to be quantified over a 36-to-50-yr. period. Peros Banhos represents one of the few atolls globally where natural island dynamics can be appraised; withstanding just one of its 35 islands, this atoll has never been settled by humans. By contrast, Diego Garcia has undergone pronounced anthropogenic change in the last fifty years. Statistics bring new insights to the persistence of these atoll islands under the contemporary conditions of sea level rise. Key findings include: (i) Coastlines facing the prevailing trade winds retreat through time, while those in leeward positions expand; (ii) coastline expansion and retreat are in balance such that total land area of all the considered islands is virtually static over the last 50 years; and, (iii) small islands (<20 ha) are substantially more dynamic than large ones. The stretches of the Diego Garcia coastline in close vicinity to human modification are more likely to suffer erosion than those situated far from human activity, and also substantially more likely to erode, than those of the uninhabited islands of Peros Banhos. A comparison between the behavior of a broad portfolio of islands spanning the Indian and Pacific Oceans emphasizes local factors such as wind direction, to be better determinants of coastline dynamics than global factors, such as the rate of eustatic sea-level rise. In aggregate, our data suggest that atoll islands are likely to persist in the face of accelerating sea-level rise over the next decades, but their high rate of coastline dynamics will challenge human habitability.

1. Introduction

Coastlines are dynamic environments. Their morphology is influenced by a host of controls, including sea level, on timescales of minutes to millennia. Not least because of our desire to live by the sea, the dynamics and drivers of coastal change have been studied intensively (Richmond, 1993; Kaluwin and Smith, 1997; Dickinson, 1999; Masselink and Pattiaratchi, 2001; Woodroffe, 2008; Collen et al., 2009; Webb and Kench, 2010; Rankey, 2011; Purkis and Klemas, 2011; Taylor and Purkis, 2012; Andréfouët et al., 2013; Purkis et al., 2016a; Duvat and Pillet, 2017; Tuck et al., 2019; Duvat, 2020; Newnham et al., 2020; Holdaway et al., 2021). Notwithstanding raised atolls, those that have been tectonically uplifted, atoll islands are low and flat with maximum elevations typically in the range of only a few meters. Being only slightly

above sea level carries several implications. First, atoll islands are vulnerable to extreme events such as storms, as well as to global environmental change – sea-level rise, in particular. On the latter point, though, it has been suggested that some (but not all) coral islands might be morphologically resilient to rising seas (Kench et al., 2005; Woodroffe, 2005, 2008; Webb and Kench, 2010; Kench et al., 2015; McLean and Kench, 2015; Beetham et al., 2017; Tuck et al., 2019), though some argue to the contrary (Hubbard et al., 2014; Storlazzi et al., 2015). In addition, atoll islands have little land area and limited natural terrestrial resources, e.g., climate-sensitive supplies of fresh groundwater (Bailey, 2015; Barkey and Bailey, 2017; Falkland and White, 2020). Finally, terrestrial plants build the base of the entire inland atoll ecosystem. The decomposition of the terrestrial plant material (leaves, stems, roots, etc.) forms a layer on the soil surface (Boberg, 2009; Coleman et al., 2017)

herein referred to as 'brown soil'. Because of its biological origin, expansion of brown soil areas will occur on timescales determined by the lifecycle of the constituent plant species. As more than 99.8% of the terrestrial plant species have a finite tolerance to salt (Flowers and Colmer, 2015), it is anticipated that repeated exposure to seawater will lead to rapid ecosystem collapse and thus 'brown soil' contraction will reflect rates of plant death and soil structure degradation.

Whereas atoll islands are rare in the tropical Atlantic, they are common in the Pacific and Indian Oceans, where they constitute entire countries or overseas territories of continental states, serve as home to hundreds of thousands of inhabitants, and house critical and strategic infrastructure. As summarized by Duvat (2019), out of 709 atoll islands which have so far been analyzed to quantify shoreline dynamics, 533 islands are located in the Pacific and only 176 in the Indian Ocean. Of the work accomplished in the Indian Ocean, the Maldives Archipelago has received the most attention (e.g., Aslam and Kench, 2017). Even from this portfolio of studies, only one (at the scale of entire atolls), Nadikdik Atoll in the Pacific, is an uninhabited site, thereby allowing for the dynamics of an anthropogenically-unaltered atoll to be observed (Ford and Kench, 2014). Although it has long been recognized that artificial modification of the coastal zone can strongly influence shoreline migration (Ford, 2012; Hamylton and East, 2012; Duvat and Pillet,
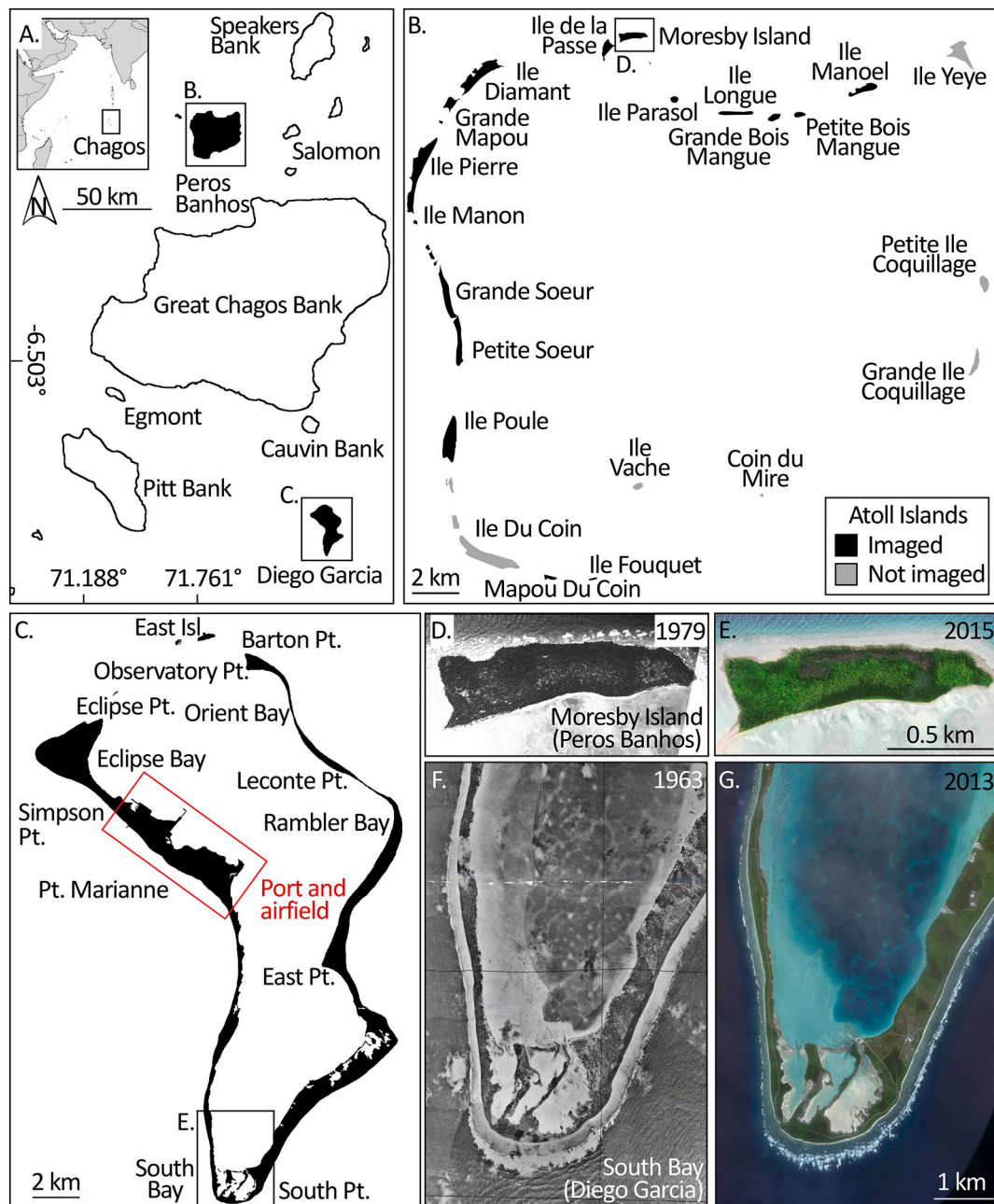

Fig. 1. (A) The Chagos Archipelago is situated in the central Indian Ocean and consists of eight isolated carbonate platforms ornamented by more than 55 individual atoll islands. This study considers two of these platforms. In the north, Peros Banhos (B) hosts 32 islands atop its reefal rim. The second site, Diego Garcia (C), is the southernmost atoll in the archipelago and ornamented by a single island which occupies the entirety of the atoll rim, except for its northern margin. The red box in (C) denotes the location of the U.S. military port and airfield complex which has been constructed on Diego Garcia in the last 50 years. Although human modification of the island has been concentrated in this sector of the atoll, infrastructure has been built elsewhere along the eastern limb of the atoll. The high fidelity of the vintage aerial photographs and modern satellite data is emphasized using representative imagery from Moresby Island, Peros Banhos, and South Bay, Diego Garcia (D-E & F-G, respectively). (For interpretation of the references to colour in this figure legend, the reader is referred to the web version of this article.)

2017; Purkis et al., 2016a), this latter study emphasizes that even atoll islands uninhabited by humans are naturally dynamic.

The paucity of studies which consider both uninhabited and inhabited islands in the same archipelago (and therefore under the same biophysical controls) frustrates efforts to disentangle the human effects of coastline erosion triggered by inappropriate intervention, such as the construction of seawalls that can starve beaches of necessary sediment supply, from natural island dynamics. A full and thorough understanding of the natural behavior of these systems in a period of relatively static sea level, as compared to the rapid rise witnessed in the Early to Mid-Holocene, can provide a critical baseline as to the lower-end of island reconfiguration that should be anticipated in the present era of accelerated sea level rise.

In this study, we assemble a suite of archive aerial photographs (negatives) for the Indian Ocean Chagos Archipelago (Fig. 1A). These photographs were acquired in the 1960's and 1970's and have an effective resolution finer than 0.2×0.2 m. In this study, we consider two atolls. First, Peros Banhos (Fig. 1B), one of the very few atolls globally where natural island dynamics can be quantified at the scale of a whole atoll – withstanding just one of the 35 islands, Peros Banhos has never been settled by humans. This atoll represents an excellent natural laboratory because its islands are near-evenly distributed around the atoll rim, thereby allowing for nuanced differences between windward and leeward positions to be examined. The second atoll considered is Diego Garcia (Fig. 1C). While the majority of the coastline of Diego Garcia is unmodified, a U.S. military port and airfield complex has been constructed in the last 50 years on the western limb of the atoll which now occupies approximately 10% of its circumference (see red box in Fig. 1C). The coastline dynamics of Diego Garcia have been considered by both Hamylton and East (2012) and Purkis et al. (2016a), and therefore the trajectory of the atoll with regard to prevailing natural and anthropogenic forcings is well understood. Capitalizing on this previous work, and expanding to include the uninhabited islands of the adjacent Peros Banhos Atoll, allows the dynamics of atoll islands in their natural state (Peros Banhos) to be contrasted with those of an anthropogenically-disturbed system (Diego Garcia), while avoiding bias introduced by varying ocean climate - both sites are closely situated in the same archipelago. The comparison is further strengthened by the subequatorial position of Chagos which prevents direct impacts by cyclones. These events can cause radical local divergence of coastline dynamics, even for closely situated islands (Kench and Brander, 2006; Ford and Kench, 2016; Duvat et al., 2017). Note, however, that the Chagos atolls, like those of the adjacent Maldives (Aslam and Kench, 2017), are exposed to distant-source swells originating in the southern Indian Ocean and therefore not wholly spared cyclonic influence. Since the southern rim of Peros Banhos is poorly developed (Fig. 1B), these swells should be anticipated to impact its lagoon, and the islands which face it, more than for Diego Garcia, which has a well-developed reef rim around the entirety of the atoll (Fig. 1C).

The goals of the study are twofold: First, using remote sensing data spanning more than 50 years, to quantify whether the islands of Peros Banhos (Fig. 1D-E), an atoll which has not been disturbed by humans, behaves differently from Diego Garcia (Fig. 1F-G). Second, using a hydrodynamic model for both atolls, to explore the physical controls driving coastline change of the two systems. Answers to such questions are urgently needed – there is reasonable doubt as to whether many atoll islands globally will remain habitable in the face of rising sea level and decreasing sediment supply resulting from the wholesale collapse of coral reef systems, as wrought by ever more frequent marine heatwaves (Le Cozannet et al., 2013; Perry and Morgan, 2017; Perry et al., 2018; Sheppard et al., 2017). Atoll islands are nourished by reef-derived detritus and so their persistence is therefore closely intertwined with the fate of the reefs that surround them.

2. The Chagos Archipelago

Chagos is part of the British Indian Ocean Territory (BIOT) and lies in the center of the Indian Ocean, occupying a southern extension of the Laccadive–Maldives Ridge (Fig. 1). There are 55 atoll islands distributed atop the eight Chagos atolls. These islands are fewer and smaller than those of the Maldives or Laccadive Archipelagos. Like atoll islands globally, the Chagos Islands are low lying (only 2–5 m above sea level) and are typical coral cays constructed of limestone with underlying freshwater lenses sustained by rainfall (Graham et al., 2009; Sheppard et al., 2012; Purkis et al., 2016a). Of the 21 Chagos islands considered by this study, including 20 islands on Peros Banhos and 1 island on Diego Garcia, only the one atop Diego Garcia Atoll is inhabited. Whereas Diego Garcia, which is situated in the southeast of Chagos, is one of the smallest atolls of the archipelago (30 sq. km), it hosts the largest emergent landmass which accounts for 60% of its total island area. By contrast, Peros Banhos Atoll covers 465 sq. km, of which only 10 sq. km is occupied by its islands, which are all situated on the atoll rim. The Chagos climate is tropical and moderated by the trade winds (Eisenhauer et al., 1999). Until very recently, the archipelago's reefs were noteworthy for their health and vitality, in no small part aided by the 2010 declaration of the Chagos Marine Protected Area, which, at the time, was the world's largest (Purkis et al., 2008; Sheppard et al., 2012). By virtue of coral bleaching, however, the Chagos reefs have suffered gravely in the last five years (Sheppard et al., 2017, 2020).

There is only one 'research-grade' tide gauge maintained in the Chagos Archipelago and this is situated on Diego Garcia. Monthly-mean data compiled by Purkis et al. (2016a) calculated the rate of relative sea-level rise (i.e. that experienced by the atoll) as 5.44 mm yr^{-1} for the period 1988–2000, and 5.96 mm yr^{-1} for the period 2003–2014. These rates of relative rise are higher than the global eustatic signal as resolved by Dunne et al. (2012) for the central Indian Ocean, which was 3.1 mm yr^{-1} for the period 1988–2011. The difference might plausibly be attributed to the tectonic subsidence of the archipelago (i.e. there is an offset of approx. 2.0 mm yr^{-1} between the rate of change of relative verses eustatic sea level). However, data archived by the Global Sea Level Observing System (GLOSS – Merrifield et al., 2009) suggest the rate of subsidence for Diego Garcia is <0.05 mm yr^{-1} over the last two decades. These geodetic data therefore suggest that the rate of sea-level rise that the archipelago is presently subjected to is substantially swifter than the global eustatic average. Tides in the Chagos are semi-diurnal with a maximum magnitude of 1.5 m.

The shallow-subsurface of the Chagos atoll-islands has yet to be examined in detail (likely because of the logistical and legal challenges of importing drilling equipment) and the genesis of the islands is therefore poorly constrained. There is not a complete deficit of data, though. Eisenhauer et al. (1999) report the fossil reefs that underlie many of the Chagos islands accumulated at a time coinciding with sea-level fall during the Mid Holocene. During this time, the relaxation of the continental crusts in glaciated areas and the reorganization of the period after the waning of the major ice caps caused a redistribution of water mass globally (e.g., sea level rises relative to Caribbean islands and fall around Indian Ocean and Australian continental margin). Conversely, Kench et al. (2005) and Perry et al. (2013) provide evidence that the atoll islands of the Maldives, analogous to those of the Chagos because of their proximity, accumulated earlier and with the sedimentary infilling of lagoons, when sea level was rising rather than falling. On the basis of the available evidence, we can be confident that the majority of the Chagos islands are "pinned" by Pleistocene and younger aged reefal deposits. Further, it is clear that after the last interglacial, coral reoccupied the raised atoll margins of both the Chagos and Maldives Archipelagos and grew vertically, keeping up with sea-level rise to deliver the morphology of the present-day atolls (Droxler and Jorry, 2021).

Almost all of the Chagos islands are covered with coconut groves (e. g., *Barringtonia asiatica, Alophyllum inopyllum,* plus *Cocos nucifera* in

Diego Garcia). Through the eighteenth and early nineteenth centuries, coconut oil became the primary produce of Chagos, whose islands then gained their characteristic skyline of palms (Fig. A.1). Throughout the archipelago, plantations caused the native vegetation to be cleared and the coconut oil became so successful that the archipelago became known as the Oil Islands, prior to the industry's collapse and abandonment of the coconut plantations. A few islands, notably on the Great Chagos Bank and Peros Banhos, remained too inaccessible for regular use and escaped coconut planting. As a result, these, typically small islands continue to boast native hardwood trees and other original plants, together with high densities of bird species which were lost from the heavily-planted islands due to the introduction of rats (Sheppard, 2016; Graham et al., 2018). Boosted by rat-eradication programs, seabird species, such as *Onychoprion fuscatus, Anous tenuirostris* and *Sula sula*, now inhabit 30 of the Chagos islands. Most of breeding seabirds are recorded in the northern and eastern Perhos Banhos islands including Ile Parasol, Ile Longue, Petite Bois Mangue, Petite Coquillage, and Grande Coquillage (McGowan et al., 2008).

3. Methods

This study was facilitated by the discovery of a collection of vintage aerial photographs acquired over Diego Garcia in 1963 and Peros Banhos in 1979. The former atoll was imaged in its entirety, whereas for Peros Banhos, several small islands in the southwest of the atoll were not photographed and therefore could not be included in our analyses (shaded gray in Fig. 1B). The workflow used to accomplish this study combined fieldwork, remote sensing, hydrodynamic modelling, and computational GIS. For the sake of brevity, a succinct overview of the methods is provided herein, with full details presented in the appendix which accompanies this publication. Figures in the appendix are identified with the prefix 'A', e.g., 'Fig. A.1′, 'A.2′, e.t.c. Equations in the appendix are similarly prefixed e.g., Eq. (A.1).

A five-step workflow was deployed to accomplish the change detection analysis for the atoll-island coastlines (Fig. 2). Under the auspices of the Global Reef Expedition accomplished by the Khaled bin Sultan Living Oceans Foundation Global (Purkis et al., 2019 for overview, 'KSLOF-GRE' hereafter), two month-long visits to the Chagos Archipelago were conducted in 2015 for the purpose of collecting field data. Alongside baseline surveys of the archipelago's reefs and associated ecosystems, real-time kinematic global positioning system (RTK-GPS) data and 3-dimensional 360° photogrammetric imagery were collected for the coastlines of the considered islands using a backpack-mounted system (Fig. A.1B). Second, the vintage aerial photographs were scanned and georectified against the RTK-GPS data collected during fieldwork. Quantification of the spatial uncertainty associated with georeferencing yielded a root mean square error of <1.0 m. Second, the modern WorldView-2 satellite images (acquired in 2013 for Diego Garcia, 2015 for Peros Banhos) were pan-sharpened to increase their spatial resolution from 2.0 m to 0.50 m per pixel. Third, GIS routines were used to extract the coastlines from the vintage aerial photographs and modern satellite imagery (Fig. A.2), which was accomplished with an error < 2.5 m.

Fourth, the coastlines of each atoll-island were partitioned according to whether they were lagoon-facing, ocean-facing, else 'hoa' facing, with the latter capturing those inter-island channel-facing shorelines which
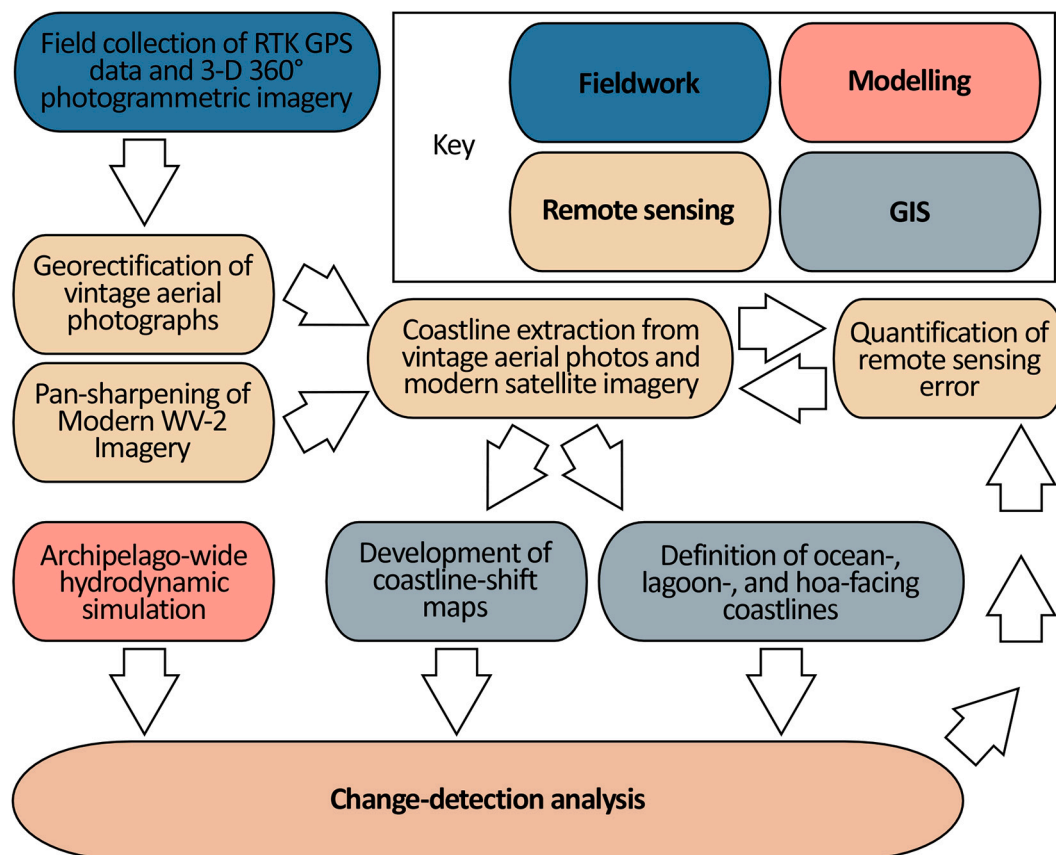

Fig. 2. Flowchart describing the methods adopted by this study which meld fieldwork, remote sensing, hydrodynamic modelling, and computational GIS to accomplish a change detection of the Chagos islands coastlines. Georectification errors in the remote sensing workflow were quantified via comparison with independent real-time kinematic (RTK) global positioning system (GPS) data collected during fieldwork. To ensure robust results, sections of coastline identified as having shifted during the period of observation were scrutinized for georectification error. If present, the images were re-rectified, the coastlines re-extracted, and the change-detection analysis repeated. Methods are fully developed in the appendix accompanying this paper.

neither face the lagoon nor the ocean (Fig. A.3). The extracted coastlines were processed into coastline-shift maps (Figs. 3, 4, & 5) to capture the behavior of the lagoon-, ocean-, and hoa-facing coastlines through time. Data from the shift maps were assembled to describe the per-island net changes in island area for the periods of observation (1963–2013 for Diego Garcia; 1979–2015 for Peros Banhos). Net areal change was also computed as a percentage of the overall size of each island, and as a rate of change, taken to be the change in island area per decade (Table 1). Aggregation of these data into stretches of ocean-facing coastlines which had been augmented by human activity, versus those far from such augmentation, allowed the influence of anthropogenic impact on coastline migration to be quantified (Fig. 6). Note that we could not conduct an equivalent test for the lagoon-facing coastlines of the atolls because fringing reefs are virtually absent from the interior of Diego Garcia, though wide and well-developed in Peros Banhos, thereby preventing a like-for-like comparison of dynamics.

Next, following the workflow described by Purkis et al. (2007), trends between the shape of the Peros Banhos islands and the behavior of their coastlines through time were explored by computing the principal axes ratio (PAX) of each island (Fig. 7). These data were considered in unison with the size of the islands. Equivalent analysis cannot be conducted for Diego Garcia since it hosts a single large island which inhabits the majority of the atoll rim.

Fifth, in order to relate coastline behavior to the prevailing ocean conditions acting on each island, a hydrodynamic model for the Chagos Archipelago was developed according to the workflows presented by Chollett and Mumby (2012), Purkis et al. (2015b), and Perry et al. (2015). This model (Eq. A.1 through A.6) was conditioned using daily wind speed and direction retrieved from QuikSCAT melded with the reef maps created by the Millennium Coral Reef-Mapping Project (Andréfouët et al., 2006; Andréfouët and Bionaz, 2021) and the KSLOF-GRE (Purkis et al., 2019). The hydrodynamic model delivers an estimated magnitude of wave energy incident on the coastlines of Peros Banhos (Fig. 8) and Diego Garcia (Fig. 9) in units of joules per m^3. Because the atoll-island coastlines are fronted by different hydrodynamic conditions, it is reasonable to assume that they will undergo variable change according to whether they face the open ocean or the lagoon. To explore this premise, the terrestrial area gained or lost over the 36 yrs. of observation was quantified for each of the 20 Peros Banhos islands for which time-separated remote sensing data exist (Fig. 10). A distinction was made between those islands which were less than 20 ha. in area at the time the atoll was imaged in 1979, and those which were larger than this threshold. Data were assembled to consider the performance of the complete island coastlines, agnostic to whether they are ocean-, lagoon, and hoa-facing (Fig. 10B), as well as each of these three categories in isolation (Fig. 10C, D, and E, respectively). The hoa-facing coastlines were not considered in the equivalent analysis for Diego Garcia since this atoll hosts a single large island and therefore lacks hoa.

Finally, the results from this study were evaluated in the context of data describing the behavior of atoll islands elsewhere in Indian and Pacific Oceans collated by Duvat (2019) (Fig. 11), and this database analyzed in the context of the differential rates of sea-level rise across these ocean basins (Fig. 12).

4. Results

4.1. Aggregate changes in the area of atoll islands for Peros Banhos and Diego Garcia

Data describing per-island net changes in area (Table 1) reveal that whereas some islands have expanded through time and others contracted, the decadal percentage changes are exceedingly small, at <1% when averaged across all of the considered islands. An outlier to this trend is Ile Fouquet (Peros Banhos), however, which contracted in area by −6.55% per decade of observation (Fig. 3A-D). This island, which is situated on the southern rim of Peros Banhos, lost 19.1% of its area from the ocean-facing coastline and 13.6% from its hoa-facing coastline between 1979 and 2015. The islands neighboring Ile Fouquet behaved in a manner consistent with the broader dataset. The net areal reduction in island area over the period of observation for the 20 uninhabited Peros Banhos islands is 0.004%, increasing to 0.900% for Diego Garcia. However, it is important to realize that these low values of net areal change computed over entire islands do not exclude the possibility of substantial coastline dynamics, such as extension in one part of an island, offset by erosion in another (e.g., Purkis et al., 2016a; Aslam and Kench, 2017). Such local nuances are captured by our separate analysis of ocean-, lagoon-, and hoa-facing coastlines. A number of recent studies have coalesced around the consensus that any change in island area < 3% of the total land area lies within the error of time-separated remote sensing (McLean and Kench, 2015; Duvat and Pillet, 2017; Duvat et al., 2017; Duvat, 2019). Placing our Chagos data in this context emphasizes the net stability of the atoll islands during the period of observation. The average areal change, however, is not representative of the high degree of coastline dynamics (Figs. 4 & 5) which can be recognized when the island coastlines are partitioned according to whether they are lagoon-, ocean-, or hoa-facing Fig. 10

Annualized average rates of coastline migration are assembled in Table 2. Of the coastlines which have expanded during the period of observation, it is those which are hoa-facing that show the highest rates of migration for Peros Banhos (average migration rate over 20 islands of 0.24 m/yr., versus 0.16 m/yr. for lagoon- and 0.18 m/yr. for ocean-facing coastlines). Of the coastlines which have retreated during the period of observation, it is those which are ocean-facing that show the highest rates of movement for Peros Banhos. The average migration rate over the 20 Peros Banhos islands for ocean-facing coastlines is −0.34 m/yr., versus −0.15 m/yr. for lagoon- and − 0.28 m/yr. for hoa-facing
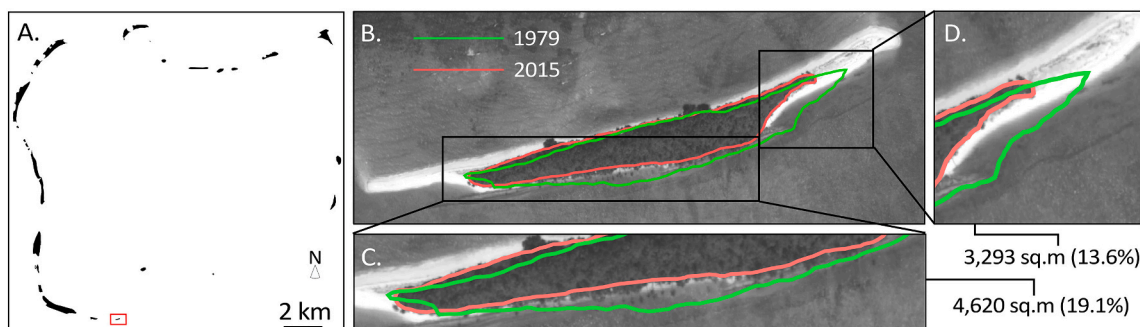

Fig. 3. Ile Fouquet, which is situated on the southern rim of Peros Banhos (A-B), lost nearly one quarter of its ocean- and hoa-facing coastlines between 1979 and 2015. The *green line* in (B) depicts the position of the coastline in 1979, whereas *orange line* depicts its position in 2015. (C) and (D) emphasize the extraordinary erosion that has occurred in the span of 36 years. The ocean-facing coastline has lost 4620 sq. m in this time period, equivalent to 58% of the area of the island. The hoa-facing coastline, (D), lost 3293 sq. m. (For interpretation of the references to colour in this figure legend, the reader is referred to the web version of this article.)
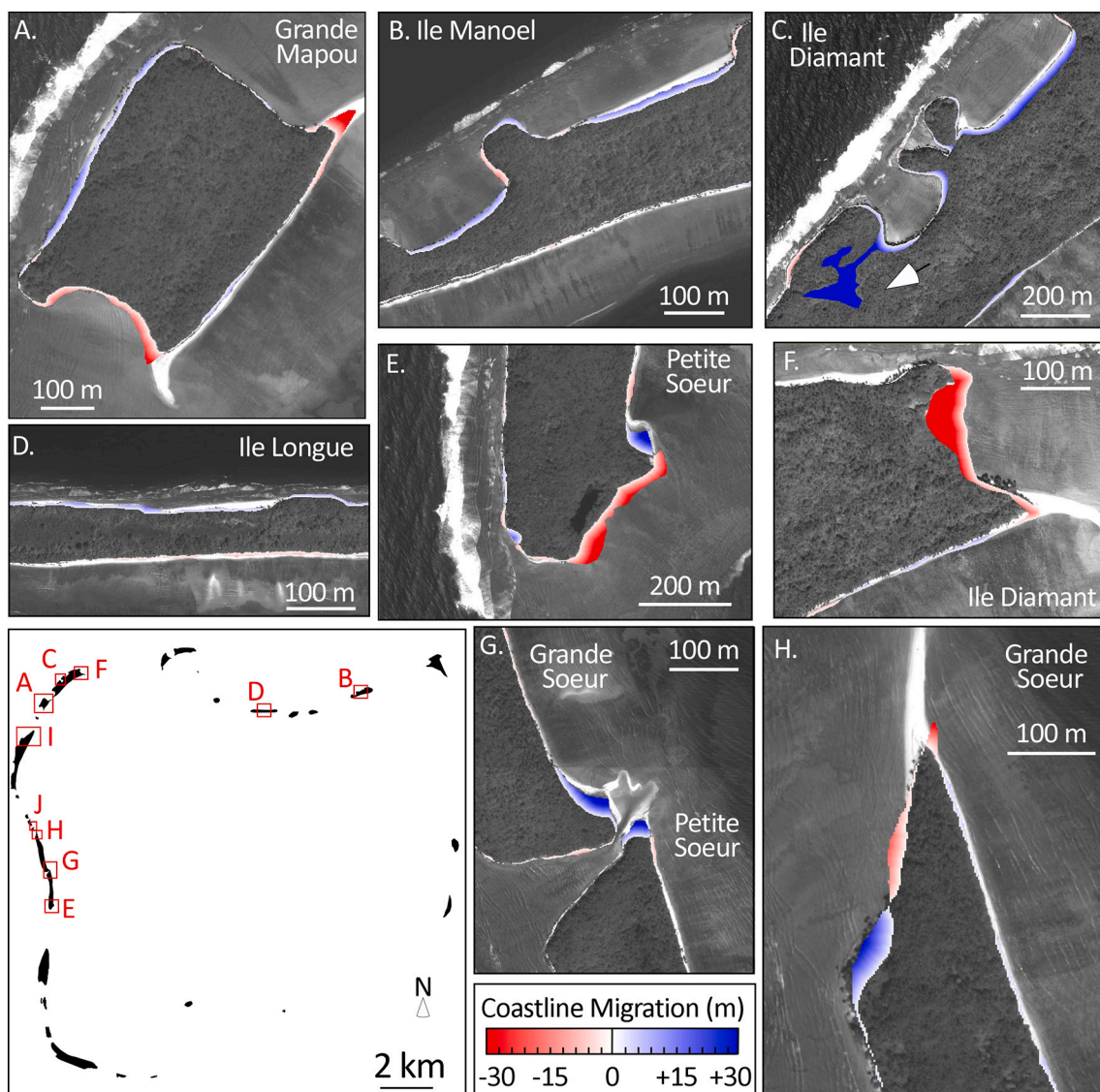
Fig. 4. Coastline-shift maps highlighting areas of land gained and lost between 1979 and 2015 for the islands of Peros Banhos. *Hot colors* denote areas of coastline retreat and *cool colors* denote expansion. Grayscale WorldView-2 satellite image acquired in 2015 is used as the base layer. (A), (B), (C) and (D) illustrate that the ocean-facing coastline of several islands distributed on the western and northern rim show pronounced expansion, which has been delivered by the beachward migration of the brown-soil line. (A) Shows the expansion of entire ocean-facing coastline, (B) and (C) are taken from the northern rim, where pronouncing expansion could be mainly found on the 'U'-shaped part of the coastline. (C) Further shows a second mechanism for the seaward expansion of an island-embayment infilling. (D) Emphasizes the overarching pattern of coastline migration in Peros Banhos whereby the ocean-facing coastline expands while the lagoon-facing coastline retreats. Meanwhile, the hoa-facing coastlines are particularly dynamic. The tips of the islands in (E) and (F) both retreated by more than 30 m. (G) Highlights the rapid accretion of sand spits. Both (A) and (H) exhibit marked erosion of island tips. (For interpretation of the references to colour in this figure legend, the reader is referred to the web version of this article.)

coastlines. As emphasized in Table 2, and in contrast to Peros Banhos, on Diego Garcia the lagoon-facing coastline has expanded more rapidly than the ocean-facing (0.27 vs. 0.21 m/yr., respectively). Rates of retreat are also more rapid on the lagoon-facing shoreline of Diego Garcia than on the island's ocean-facing shoreline at 0.37 m/yr. and 0.25 m/yr., respectively. In aggregate, these data suggest the lagoon-facing coast to be considerably more dynamic than the ocean-facing side. This said, and as emphasized by Purkis et al. (2016a), the most dynamic precinct of Diego Garcia is the lagoonal embayments in the south of the atoll (emphasized in Fig. 5B). However, the dynamic behavior of these embayments serve to mask lethargic coastline changes elsewhere on Diego Garcia. For instance, recomputing annualized changes for this atoll island with its southern embayments omitted, reveals the lagoon-facing coastline to be retreating more slowly than the ocean-facing coastline (−0.02 m/yr. vs. -0.06 m/yr., respectively). When the degree of

expansion and retreat is averaged across all the islands of Peros Banhos, and across Diego Garcia, both atolls emphasize that the total land area is almost static over the period of observation because area lost is nearly balanced by area gained. The net annualized rate of change is −0.02 m/yr. for Peros Banhos and − 0.07 m/yr. for Diego Garcia.

Table 2 reveals that the ocean-facing coastlines of the Peros Banhos islands display the highest rates of retreat. Analysis of individual islands, however, shows that not all ocean-facing coastlines on this atoll have retreated in the considered time period. For instance, sectors of the ocean-facing coastline of several islands distributed on the western and northern rim of the atoll show pronounced expansion (Fig. 4A, B, C, and D). Examination of the time-separated remote sensing imagery reveals that these areas of coastline expansion have been delivered by the beachward migration of the brown-soil line, presumably driven by the conversion of beach sands to vegetated island interior. This mechanism,
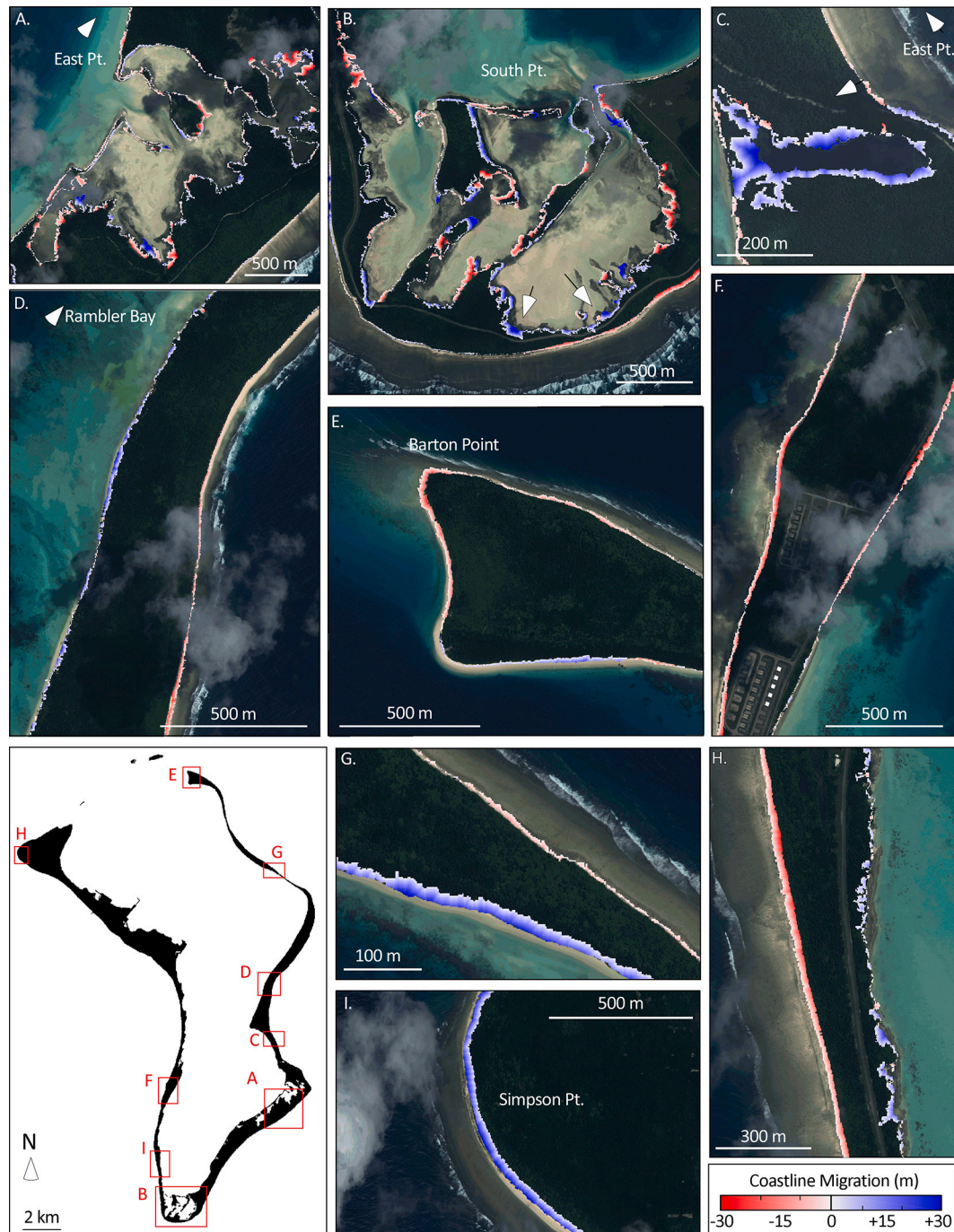
Fig. 5. Coastline-shift maps highlighting areas of land gain (*blue*) and loss (*red*) between 1963 and 2013 in Diego Garcia. High-resolution true-colour satellite imagery acquired in 2013 is used as the base layer. (A) through (C) illustrate how tranquil embayments on the lagoon-facing coastline of the island are highly dynamic and swiftly infill through time, thereby increasing the area of the island. Cases of land lost on Diego Garcia tend to be on ocean-facing coastlines (D, E, F,G, and H). In rare cases, however, ocean-facing coastlines do prograde seaward, such as resolved in (I), accompanied by a loss of land on the lagoon side. Here, the seaward expansion of Simpson Point is particularly pronounced. (For interpretation of the references to colour in this figure legend, the reader is referred to the web version of this article.)

which has expanded islands by as much as 15–20 m in the last half-century, is particularly important on the islands which ornament the western rim of Peros Banhos, such as Grande Mapou (Fig. 4A). For islands on the northern rim of this atoll, this mechanism of island growth is also present, but restricted to ocean-facing embayments, such as exist on Ile Manoel (Fig. 4B) and Ile Diamant (Fig. 4C). Ile Diamant shows an additional mechanism of growth. Here, the area behind a promontory on the ocean-facing side of the island which existed in 1979 has completely infilled by 2015, serving to expand the island by >30 m (white arrow in

Fig. 4C). By contrast to the dynamic ocean-facing coastlines of Peros Banhos, the lagoon-facing coastlines are all very stable. If change can be detected, however, it tends to be a modest retreat (such as observed for Ile Longue, Fig. 4D). Such inactivity is lacking for the hoa-facing coastlines of the Peros Banhos islands which are particularly dynamic. For instance, the tips of the islands of both Petit Soeur (Fig. 4E) and Ile Diamant (Fig. 4F) both retreated by more than 30 m in the period of observation. Further, the rapid accretion of island tips caused the hoa-facing coastlines of other islands to expand considerably – particularly

Table 1
Summary of the behavior of the 21 considered islands in the Chagos Archipelago.

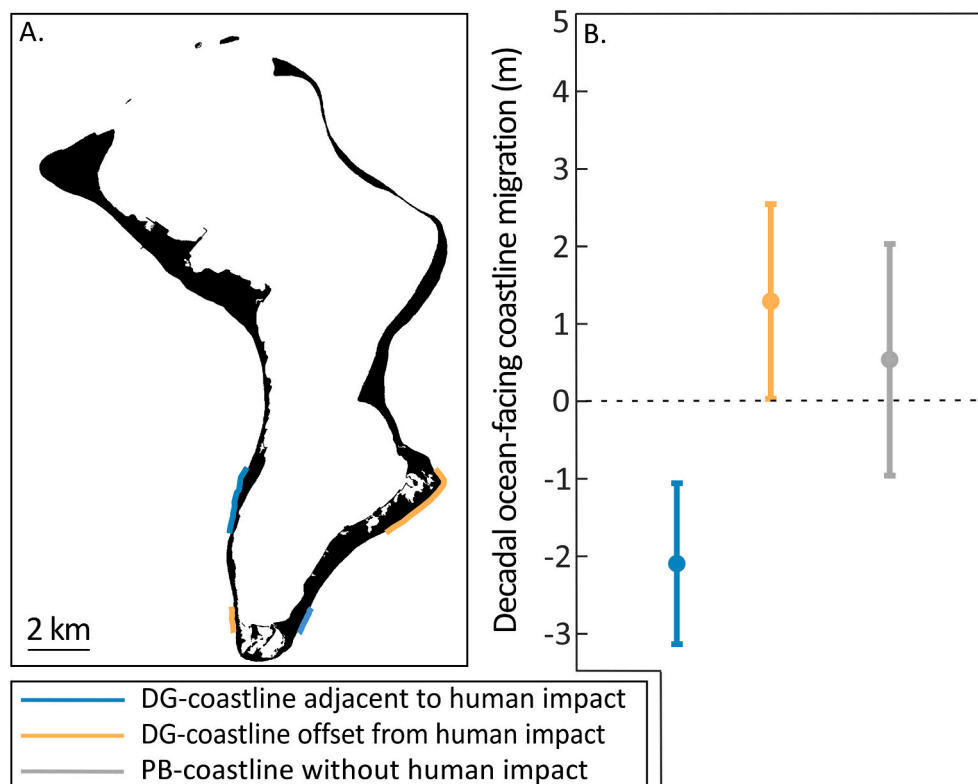| Atoll	Island	Island Area (ha.)	Net Areal Change (ha.) (%)		Decadal Areal Change (%)	Time Period	Average Areal Change %
Peros Banhos	Petite Mapou	1.10	−0.03	−3.07	−0.85	1979–2015	−0.004
	Ile Finon	1.27	−0.03	−2.09	−0.58		
	Ile Fouquet	1.85	−0.57	−23.58	−6.55		
	Ile Manon	2.20	0.04	1.74	0.48		
	Unnamed Island	2.40	−0.07	−2.67	−0.74		
	Ile Verte	3.75	0.04	0.97	0.27		
	Mapou du Coin	6.74	0.14	2.15	0.60		
	Ile Parasol	7.74	0.11	1.50	0.42		
	Petite Bois Mangue	8.01	0.06	0.08	0.22		
	Grande Bois Mangue	11.83	0.23	1.99	0.55		
	Ile Longue	17.81	0.28	1.62	0.45		
	Grande Mapou	18.74	−0.06	−0.34	−0.09		
	Ile Passe	20.69	−0.21	−1.00	−0.28		
	Ile Manoel	29.40	0.15	0.51	0.14		
	Moresby Island	30.87	1.31	4.44	1.23		
	Petite Soeur	46.22	−0.85	−1.81	−0.50		
	Grande Soeur	55.24	−0.19	−0.35	−0.10		
	Ile Diamant	83.26	1.72	2.11	0.59		
	Ile Poule	89.31	−1.18	−1.31	−0.36		
	Ile Pierre	118.12	−0.92	−0.77	−0.21		
Diego Garcia	–	2124	−19.49	−0.90	−0.18	1963–2013	−0.900

Fig. 6. Human impact on coastline erosion. Three categories of coastline were considered between the two atolls. (A) Stretches far from human modification on both Diego Garcia ('DG', orange) and Peros Banhos ('PB', gray), and stretches of coastline in the immediate vicinity of human modification on Diego Garcia (blue). (B) Shows the average coastline migration per decade of the three categories. Error bars denote one standard deviation around the mean. The behavior of the coastline in the vicinity of human activity on Diego Garcia is significantly different ($p = 0.05$) to that of the undisturbed stretches on the same atoll and those considered from Peros Banhos – text for details. (For interpretation of the references to colour in this figure legend, the reader is referred to the web version of this article.)

so for highly elongate islands such as Grande and Petite Soeur (Fig. 4G). Tips can also radically decrease in size through time (e.g., Fig. 4A - Grande Mapou and Fig. 4H - Grande Soeur).

Switching attention to Diego Garcia, local examples of both expansion and retreat of the ocean- and lagoon-facing coastlines alike can be identified in the time-separated remote sensing data (Fig. 5). Although the filling of embayments is a rare motif of coastline advance for the Peros Banhos islands, it is a common mechanism of growth on the lagoon-facing side of Diego Garcia. As can be illustrated with the remote sensing imagery, many of the cuspate embayments which perforate the lagoon-facing margin of this island have infilled between 1963 and 2013 (Fig. 5A, B, and C), suggesting this mechanism to be important for the

evolution of Diego Garcia, as captured in Table 2 which emphasizes how the annualized rate of coastline migration decreases markedly for Diego Garcia if its southern embayments are not included in the analysis (0.08 vs. 0.02 m/yr., respectively). When land is gained on the lagoon-facing side of Diego Garcia, it is typically balanced by land lost on the ocean-facing side, as emphasized in the vicinity of Rambler Bay (Fig. 5D). Similarly, Barton Point (Fig. 5E), situated in the north of the atoll, has lost approximately 15 m of its ocean-facing coastline in the last 50 years (Fig. 5E), balanced by an equivalent extension of the lagoon-facing coastline. The western limb of the island in the south (Fig. 5F and H) and narrow eastern limb of the mid-island (Fig. 5G) also show the common pattern of land lost from the ocean-facing coastline and minor
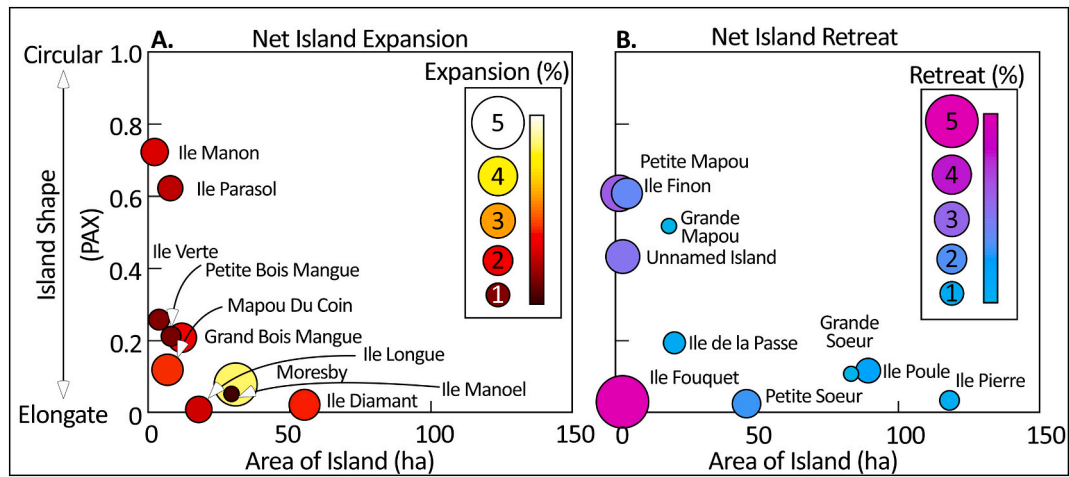
Fig. 7. Trends in coastline migration versus island shape and size for Peros Banhos. (A) Plots the 10 islands that have expanded in area between 1979 and 2015, whereas (B) considers those which have contracted. Note consistency in behavior for both cases – circular islands are less dynamic than those which have an elongate shape. The propensity of an island's coastline to migrate is unrelated to its size.
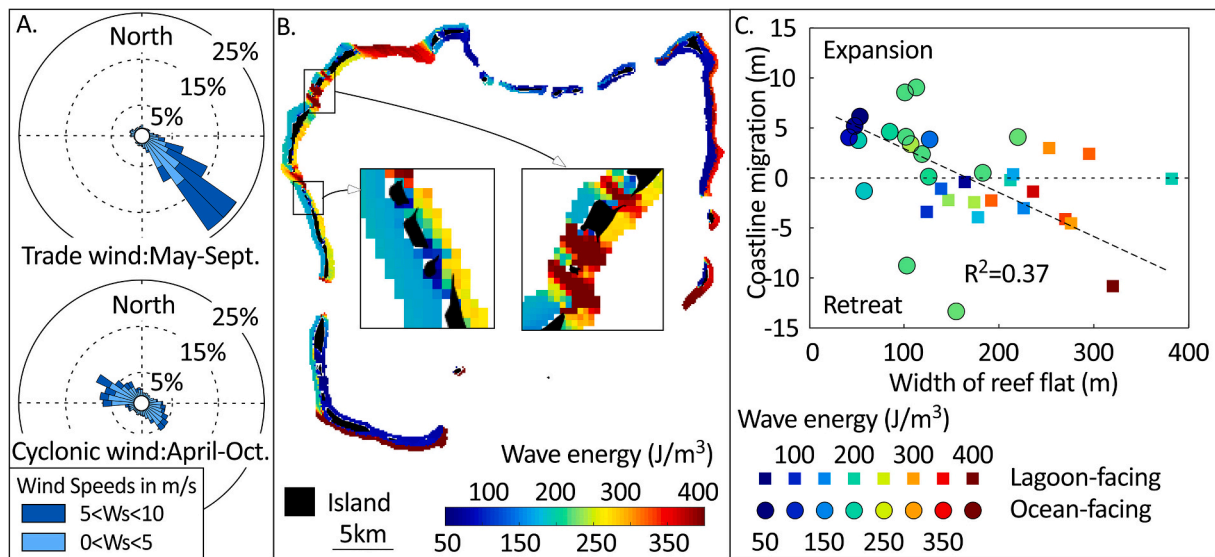

Fig. 8. Hydrodynamic energy as a driver of coastline change of the 20 Peros Banhos islands. (A) A pair of seasonal wind roses capturing prevailing wind speed and direction from the naval air station on Diego Garcia for the period 2004 through 2015. (B) Map of modelled seasonal local wave energy incident on the ocean- and lagoon-facing coastlines of the Peros Banhos. Insets emphasize that for the west of the atoll, the trade winds deliver higher energies on the lagoon-facing island coastlines than those which are ocean facing. (C) Plots coastline migration for the period 1979–2015 versus reef-flat width. The wave energy incident on each coastline is denoted in colour and circles denote ocean-facing coastlines and squares lagoon-facing. More energetic coastlines are fronted by wide reef flats and retreat through time.

gains on the lagoon-facing side. As always, however, there are exceptions to the rule with pronounced retreat recorded on both ocean- and lagoon-facing coastlines, as documented around Simpson Point (Fig. 5I).

4.2. Impact of human-population density on coastline dynamics

Comparing rates of coastline change for select portions of the ocean-facing coastlines of Peros Banhos, which are uninfluenced by human activity, to those of Diego Garcia, which have locally been augmented artificially, exposes pronounced differences (Fig. 6). Stretches of coastline offset from human impacts in both Diego Garcia and Peros Banhos (Categories [1] & [2] – appendix for details) have tended to expand at an average rate of 1.0 m per decade. By contrast, the stretches of coastline in the vicinity of human disturbance on Diego Garcia (Category [3] – see appendix) have retreated at a rate of approximately −2.0 m per decade. The behaviors of the unimpacted versus impacted coastlines are statistically different ($p = 0.05$).

4.3. Coastline dynamics vary as a function of island shape and size

Of the 20 Peros Banhos islands for which we have data, exactly half display an increase in island area over the 36 years of observation (Fig. 7A), and ten show a decrease in size (Fig. 7B). To the former, no systematic behavior is seen between the size of an island and its coastline dynamics. More circular islands, however, tend to have limited expansion, whereas those which are more elongate are more dynamic. The same trend is seen for the islands that have reduced in size (Fig. 7B).

4.4. Hydrodynamic setting of Peros Banhos and Diego Garcia

As captured by the meteorological station at the Diego Garcia airfield (from 2004 to 2015), the Chagos Archipelago is situated in the trade-
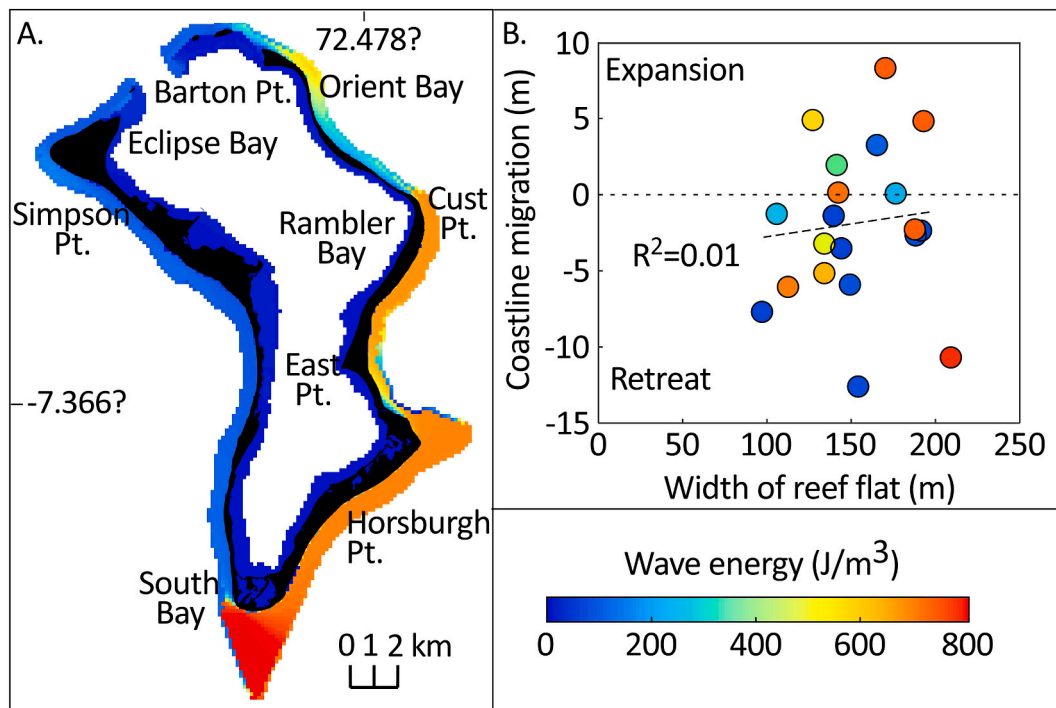
Fig. 9. The hydrodynamic setting of Diego Garcia. (A) Map of modelled wave energy incident on the ocean-facing coastlines of the island. (B) Plots of coastline migration for the period 1963–2013 (y-axis) versus reef-flat width (x-axis). The wave energy incident on each coastline is denoted in colour and circles denote ocean-facing coastlines. Unlike the case for Peros Banhos, there is no clear relationship between the hydrodynamic energy incident on the coastline of Diego Garcia, the width of the reef flat, and the change in island size through time.

wind belt from May to September during which time the wind blows strongly from the southeast. Low-velocity cyclonic winds characterize the rest of the year, during which time there is no dominant wind direction (Fig. 8A). To Peros Banhos first – the modelled hydrodynamic setting suggests that for the west side of this atoll, the trade winds deliver higher energies on the lagoon-facing island coastlines than those which are ocean facing. Here the hoa host a very high hydrodynamic energy regime, which allow sediment fluxes from ocean to lagoon, likely also *vica versa*, and thus influence nearby coastline change. Meanwhile in the northwest of Peros Banhos, energies on the lagoon-facing islands are also higher than on the ocean facing, but, because the hoa are aligned parallel with axis of the trade winds, their hydrodynamics are particularly amplified. When interpreting these data, it must be remembered that the coastlines experience prevailing wave energy after it has been attenuated by the reef flats which fringe each island and steep fore reef (Sheppard et al., 2005; Quataert et al., 2015). It is therefore imperative to also consider the width of the reef flat which was quantified from satellite imagery. Here, there is a negative relationship ($R^2 = 0.37$) between the magnitude of coastline change (1979–2015) for the 20 Peros Banhos islands, reef-flat width, and prevailing wave energy (Fig. 8C). This positive relationship, albeit weak, suggests that more energetic coastlines tend to be fronted by wide reef flats, and retreat through time. Also emphasized is that the ocean-facing coastlines of the Peros Banhos islands tend to expand through time, while the lagoon-facing retreat, as confirmed by time-separated remote sensing (Fig. 10).

The map of simulated wave energy for Diego Garcia (Fig. 9) has similarities, but also important differences, to that produced for Peros Banhos (Fig. 8). In terms of similarities, the prevailing wave energy in the Chagos, driven by the trade winds, delivers the maximum hydrodynamic energy to the southeast-facing coastline of the atoll island, as it does for the islands of Peros Banhos. The difference is that for Peros Banhos, the most energetic coastlines are lagoon-facing as the atoll's protective reef rim is most poorly developed in its southeastern quadrant (see Fig. 1B). Meanwhile for Diego Garcia, which has a well-developed

reef rim around the entirety of the atoll, save for a small hoa at its northern tip (the leeward side of the atoll), the lagoon is modelled to be quiescent, receiving zero impact from prevailing long-period ocean swell, which is instead concentrated on the ocean-facing coastlines of the island, and those which face southeast, in particular. Configured as such, it might be anticipated that the southeast-facing oceanward coastline of Diego Garcia would be particularly vulnerable to erosion. Indeed, results published by Purkis et al. (2016a) showed that this coastline has retreated during the period of observation, but only modestly so (see their Fig. 9). This behavior for Diego Garcia is in contrast to that of Peros Banhos, where there is no clear relationship between wave energy and coastline dynamics, regardless of the width of the island-sheltering reef flat (Fig. 9B).

4.5. Spatial patterns of coastline change in Peros Banhos

When the entire coastlines of the islands are considered in aggregate (Fig. 10B), it is revealed that the islands situated in the north of Peros Banhos Atoll are all increasing in size, save for Ile de la Passe (#12 in the figure) whose coastline is retreating. By contrast, all of the islands situated on the west of the atoll lost area between 1979 and 2015. If only the ocean-facing island coastlines are considered (Fig. 10C), 15 out of 20 islands, regardless of their position on the atoll rim, have gained in area. The five exceptions to this trend are Ile Pierre (#4 in the figure), Ile Poule (#11), Ile de la Passe (#12), Mapou Du Coin (#19), and Ile Fouquet (#20). The opposite trend is observed for the lagoon-facing coastlines (Fig. 10D), the majority of which have lost area. Similarly, the hoa-facing coastlines also tend to decrease in area, regardless of position on the atoll (Fig. 10E).

5. Discussion

Pairing the two sites in the same archipelago allows the dynamics of atoll islands to be contrasted while avoiding bias introduced by varying
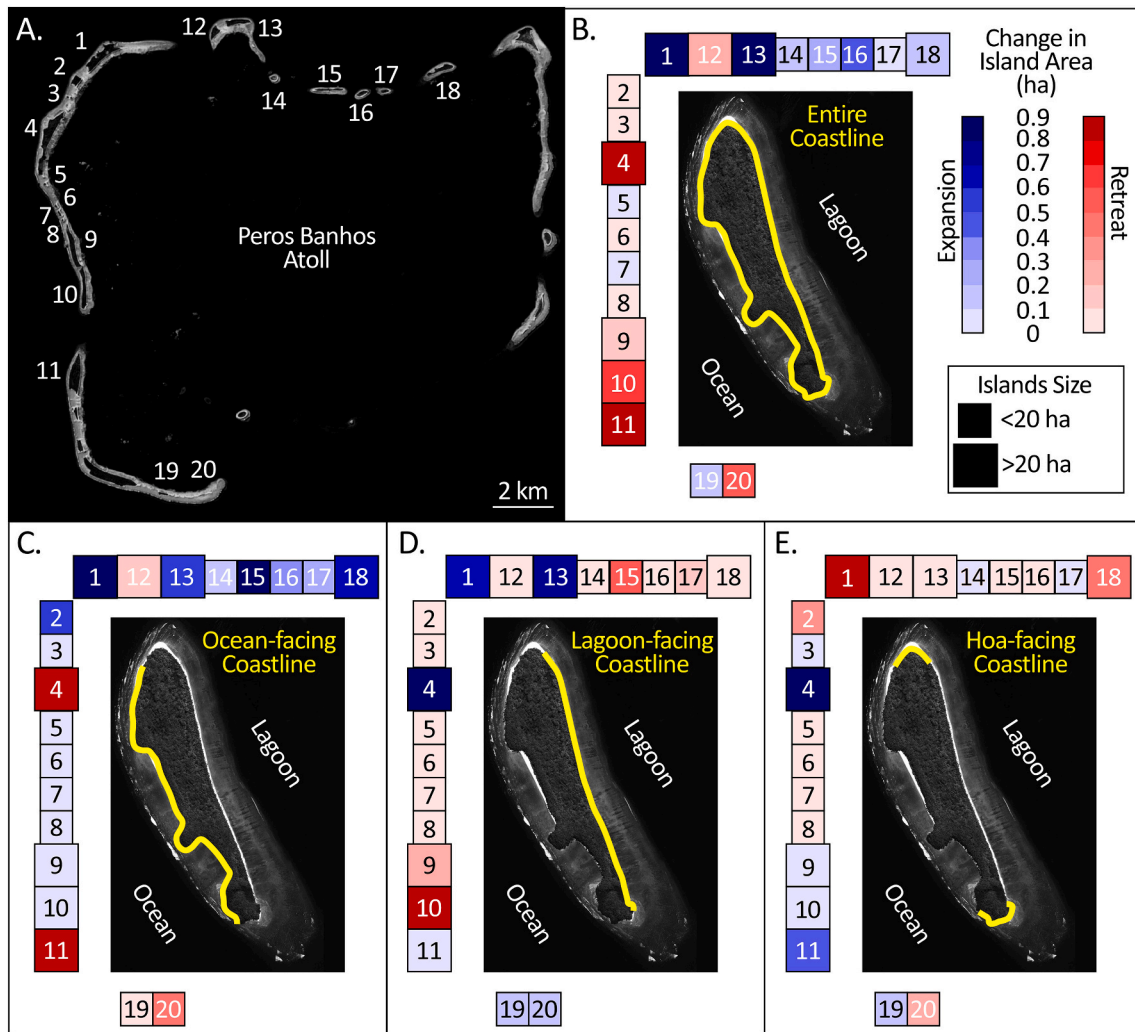
Fig. 10. Differential behavior of island coastlines for Peros Banhos. (A) Satellite image of Peros Banhos Atoll. Each atoll island for which paired remote sensing data exist is given a unique integer-identifying code. For instance, Ile Diamant in the northwest of the atoll is assigned the number '1', Grande Mapou '2', and so on. These integers provide a key for the islands in (B) through (E) which have been abstracted to squares for ease of interpretation. Per the key in (B), small squares represent islands which are <20 ha. in area, whereas the larger squares represent those >20 ha. The colour of the squares encodes the degree of expansion (*blue*) or retreat (*red*) of each island over the period of observation. (B) Describes the behavior of the entirety of the island coastlines, whereas (C) considers only ocean-facing coastlines, (D) lagoon-facing, and (E) hoa-facing. (For interpretation of the references to colour in this figure legend, the reader is referred to the web version of this article.)

ocean climate. The atolls of Diego Garcia and Peros Banhos are geomorphologically and hydrodynamically different, which delivers dissimilar styles of sediment transport, and therefore different coastline dynamics. However, at a high level, the behavior of the islands on the two atolls is similar in the sense that total island area is almost static through the half-century of observation (Table 1). In neither case, though, are the coastlines of these islands immobile. In fact, they are highly dynamic, but the island area lost is almost exactly balanced by area gained, during the period of observation. These similarities, however, mask pronounced differences in the style of island dynamics between Peros Banhos and Diego Garcia. For the former, island expansion is mediated by extension of the ocean-facing coastlines and retreat by the erosion of the lagoon-facing coastlines. This pattern is opposite to that of Diego Garcia, which sees substantial land gained on the lagoon-facing side of the island and lost on the ocean facing.

Models of hydrodynamic exposure aid in the explanation of these trends. Despite occupying the platform interior, the Peros Banhos lagoon is far from tranquil because the rim of this atoll is not competent in its southeastern quadrant, allowing long-period ocean swell to enter the lagoon, driven by the southeasterly trade winds which prevail from May through September (Fig. 8). The lagoon-facing fringing reefs excellently

emphasize the vigorous hydrodynamics within the lagoon – they represent a rare example of platform-interior reefs that have developed pronounced spur-and-groove morphology (Sheppard, 1981). Fronting this hydrodynamic energy, the lagoon-facing coastlines of the Peros Banhos islands retreat, whereas the ocean-facing ones, situated in a relative lee during the trade-wind season, expand, as sediment is hydrodynamically moved down wind. Despite being a smaller atoll than Peros Banhos, the geomorphology of Diego Garcia also differs substantially. Diego Garcia is unusual in the length and continuity of its reef rim, which extends around 90% of the atoll circumference, save only for a limited aperture on its northern face, as originally reported by Stoddart (1971). This configuration delivers a quiescent lagoon environment (Fig. 9), and, accordingly, the majority of coastline extension is witnessed on the tranquil lagoon-facing coastline of this island (Fig. 5). The retreat of Peros Banhos lagoon-facing coastlines is consistent with the observations of Rankey (2011) who noted lagoon-facing coastlines were more dynamic than ocean-facing ones for some atolls (Maiana, Aranuka) in the Gilbert Islands (Kiribati). This occurs because the lagoon-facing coastlines lacked the stabilization of well-developed fringing reefs, as present on the ocean-facing coastlines of the islands. No doubt overprinting the influence of prevailing hydrodynamics on the recent
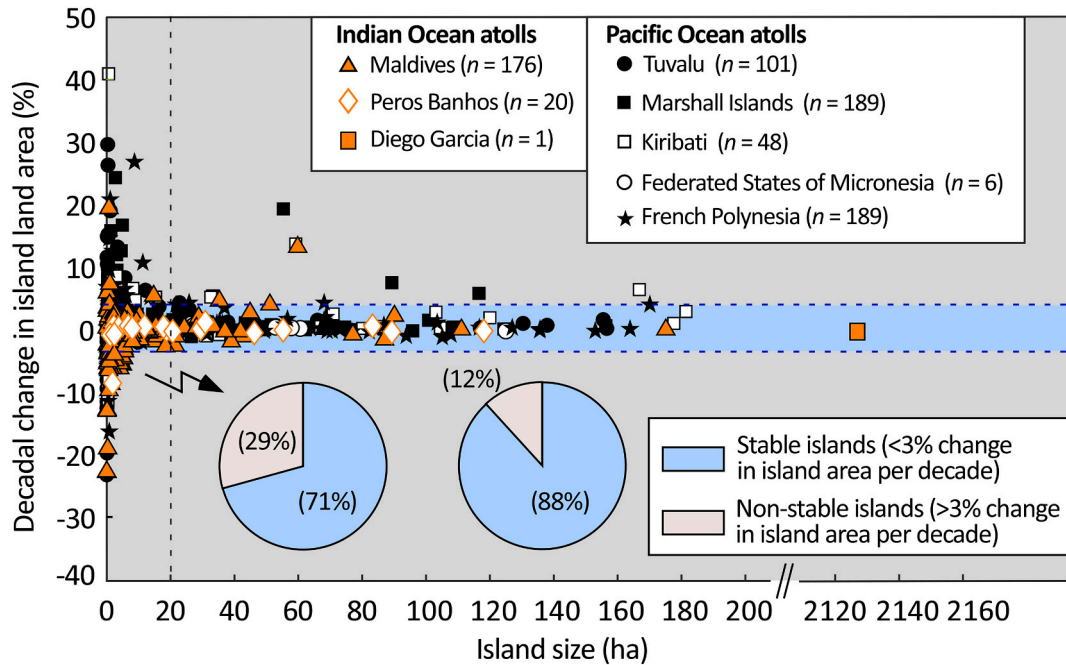
Fig. 11. A compilation of data describing the behavior of atoll islands in the Indian and Pacific Oceans (*y*-axis) versus size of those islands (*x*-axis) as collated by Duvat (2019). Any decadal change in area less than 3% of the total island area (*blue zone* bounded by dashed-horizontal *blue lines*) is generally considered as not representing a meaningful change – text for details. The *vertical dashed black line* separates the 559 islands <20 ha. in area versus the 171 islands larger than this threshold. The pie charts specify that 71% of islands <20 ha. do not meet the 3% criterion for meaningful change, which increases to 88% for those islands >20 ha. Regardless of ocean basin and biogeophysical setting, small islands are considerably more dynamic than large, a trend to which our data for this Chagos study also adhere (*orange symbols*). (For interpretation of the references to colour in this figure legend, the reader is referred to the web version of this article.)
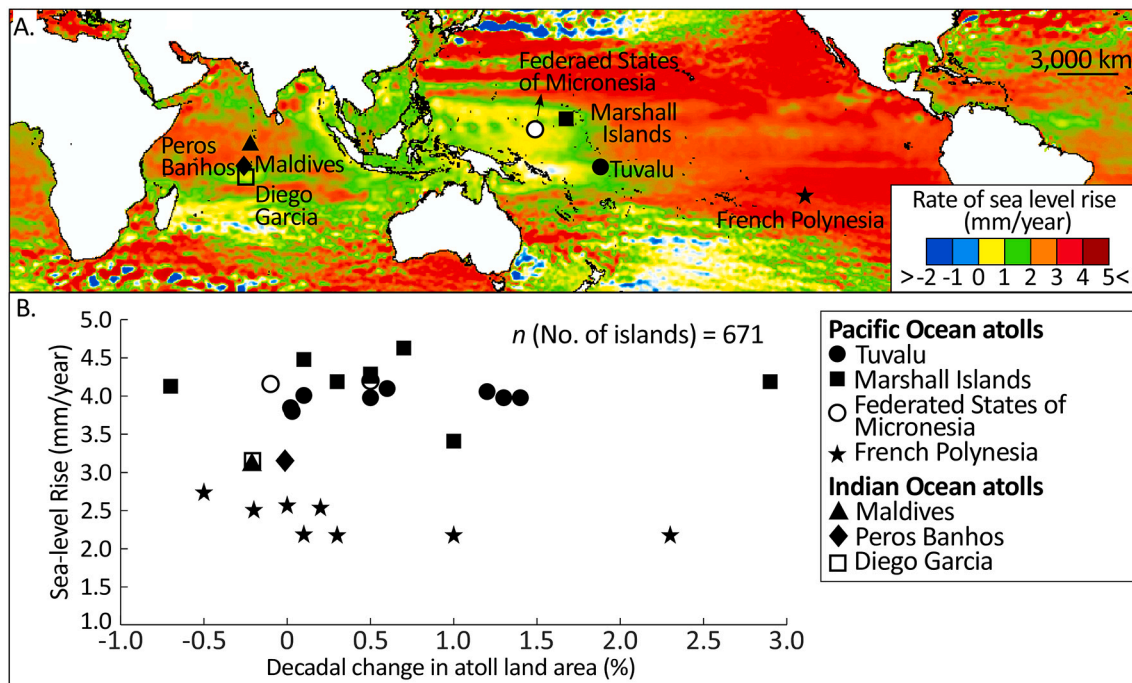

Fig. 12. (A) Map of rates of sea-level rise for the tropical and subtropical oceans compiled by the data from satellite altimetry for the years 1993 through 2018 (AVISO). *Hot colors* denote rapid rates of rise and *cool colors* emphasize negative rates of rise (sea-level fall). Plotted in (B) is the rate of sea-level rise for the waters offshore the considered atoll islands versus their decadal change in area. Note lack of correlation between the two variables, suggesting local factors to be a more important determinant of atoll-island dynamics in the considered time period than change in eustatic sea level.

evolution of the Chagos coastlines is the effect of the December 2004 Indian Ocean tsunami induced by the Sumatra–Andaman earthquake. As reported by Sheppard (2007), accounts from residents of Diego Garcia

and visitors on yachts intimated amplified tidal ranges on the day of the tsunami, though subsequent field assessment suggested local destruction of vegetation on some atolls and modification of beach profiles.

Table 2
Annualized rates of coastline change for Peros Banhos for the period 1979–2015 and for Diego Garcia (1963–2013) as determined from time-separated remote sensing.

	Migration Rate	Entire Atoll	Ocean-facing Coast	Lagoon-facing Coast		Hoa-facing Coast
		m/yr.	m/yr.	m/yr.		m/yr.
Peros Banhos	Average change net	−0.02	−0.04	−0.001		−0.008
	Average change expansion	0.18	0.18	0.160		0.240
	Average change retreat	−0.24	−0.34	−0.150		−0.280
Diego Garcia	Average change net	−0.07	−0.06	Entire Coastline[1]	Normal Coastline[2]	–
				−0.08	−0.02	
	Average change expansion	0.25	0.21	0.27	0.16	–
	Average change retreat	−0.33	−0.25	−0.37	−0.17	–

For Diego Garcia, [1]entire coastline including southern embayments and [2]excluding embayments.

Disentangling the influence of the 2004 tsunami from the fair-weather evolution of the coastline lies beyond the scope of this paper, but the contribution of the tsunami was clearly localized and comparatively modest.

5.1. Attempt for unraveling anthropogenic impact on island behavior

By comparing Peros Banhos, which is unsettled by humans, to Diego Garcia, which hosts between 1000 and 5000 U.S. troops and civilian support staff, there is the opportunity to gain insight into anthropogenic influence on atoll-island dynamics. For Diego Garcia, Purkis et al. (2016a) had previously examined the within-atoll influence of humans on coastline migration. The authors concluded that the areas suffering the most acute erosion correlated with those with the highest density of infrastructure, including areas where the coastline has been armored with concrete, etc., such as has been implemented at Simpson Point, Point Marianne, and Eclipse Point. After controlling for the abatement of wave energy by reef flats (appendix for details), this study reveals that stretches of coastline offset from human impacts in both Diego Garcia and Peros Banhos expand, whereas stretches in the vicinity of human disturbance on Diego Garcia retreat (Fig. 6). Furthermore, the difference between the two is significantly significant ($p = 0.05$). These findings suggest that human disturbance has the capability to accelerate coastline erosion in the Chagos Archipelago. Ford (2012) ascribed similarly enhanced erosion of disturbed stretches of atoll-island coastlines in Majuro Atoll, Marshall Islands, in the Pacific to reduced rates of calcification of the offshore reefal and foraminiferal assemblages, likely caused by increased turbidity and nutrient loading imposed by human activity. Such an explanation can unlikely be ported to Diego Garcia, as this atoll is generally well flushed and boasts good water quality (Sheehan et al., 2019), despite its human habitation. Accordingly, Purkis et al. (2016a) attributed the accelerated erosion of Diego Garcia to the construction of revetments and local armoring of the atoll's beaches using concrete, which serve to disrupt the natural long-shore redistribution of sediment.

5.2. The behavior of the Chagos islands is consistent with atoll islands globally

The behavior of the Chagos islands can be placed in a global context via comparison with equivalent studies which capture coastline dynamics for select islands in French Polynesia (Le Cozannet et al., 2013; Yates et al., 2013; Duvat and Pillet, 2017; Duvat et al., 2017), Tuvalu (Kench et al., 2015, 2018), the Marshall Islands (Collen et al., 2009; Ford, 2012; Ford, 2013; Ford and Kench, 2015), Kiribati (Biribo and Woodroffe, 2013; Rankey, 2011), and the Federated States of Micronesia (Webb and Kench, 2010) and one study from the Maldives in the Indian Ocean (Aslam and Kench, 2017). A common thread through the majority of these studies is that per-decade changes in island area equivalent to 3% of the total island area, or less, are considered inconsequential, which is a threshold also adopted for this comparison (Fig. 11 – islands with areas that change <3% per decade plot between the two horizontal dashed blue lines). To aid the comparison, a threshold in total island size of 20 ha. (vertical dashed black line in Fig. 11) was useful for distinguishing differences in island dynamics. For the 559 islands that are <20 ha. in area, 29% exhibit a decadal change exceeding 3% of their total area. For the >20 ha. islands, of which there are 171, only 12% exceed this threshold in dynamics. As emphasized in Fig. 11, adding the Chagos to this database shows its islands to perform within the bounds of those from the nearby Maldives Archipelago. More generally, such consistency between the two ocean basins is surprising given the varied oceanographic forcings, differences in diversity of sediment producers – including disturbances to those producers in terms of coral bleaching, etc., and perhaps most intriguingly, differences in frequency of impacts from storms and cyclones (Perry et al., 2011; Le Cozannet et al., 2013; Yates et al., 2013; Duvat et al., 2017). This consistency in behavior carries at least two important lessons. First, it reaffirms that the coastlines of small islands are particularly dynamic, though as emphasized in Fig. 11, the probability of perceptible erosion is approximately equal to the chance of island growth. Second, there seems to be universal bounds to the extent of coastline dynamics, regardless of the physical and environmental setting of the atoll islands.

5.3. Rate of sea-level rise is a poor predictor of atoll-island behavior in the Chagos and beyond

There are many reasons why rate of sea-level rise might impart control on atoll-island behavior, but two stand out. The first reason is that high rates of rise would be anticipated to amplify the hydrodynamic energy incident on coastlines, particularly so during storms, thereby increasing their erosion (Roy and Connell, 1991; Dickinson, 1999; Sheppard et al., 2005; Woodroffe, 2008; Church et al., 2006; Nicholls and Cazenave, 2010). Second, rapid sea-level rise decreases the ability of key carbonate producers to create sediment by virtue of the link between solar irradiance and production rates (Schlager, 1993; Van Woesik and Cacciapaglia, 2018) and islands starved of sediment are also more dynamic (Perry et al., 2011; Morgan and Kench, 2016). Indeed, tropical coastlines will likely become more dynamic into the future as the reefs which front them are further decimated by ocean heatwaves, tipping their carbonate budgets into negative territory (Le Cozannet et al., 2013; Januchowski-Hartley et al., 2017; Perry and Morgan, 2017; Perry et al., 2018; Ryan et al., 2019). Over the 36-to-50-yr. period of observation, however, sea-level control on island behavior is not upheld by data. Fig. 12A captures global rates of sea-level rise averaged over the period 1993 to 2018 as provided by the French Archiving, Validation and Interpretation of Satellite Oceanographic data program (AVISO) using satellite altimetry (T/P and Jason1/2/3, plus available ERS-1/2, Saral, and Envisat). The atoll islands in the Indian and Pacific Oceans for which there exists data on coastline behavior span a broad range in rates of sea-level rise (Fig. 12B). For instance, Tuvalu and the Marshall Islands are experiencing double the rate of rise experienced in French Polynesia (4 mm yr^{-1}. vs. 2 mm yr^{-1}., respectively). Decadal change in atoll-island landmass is, however, uncorrelated with rate of sea-level rise, suggesting that local factors are the primary determinants of these dynamics, at

least for the seven atoll systems (including 671 islands) assembled in Fig. 12, over geologically short timescales.

Although not prime focus of this paper, these results are relevant to the development of isolated carbonate platforms, such as the Chagos Archipelago, through geological time. Here, considerable attention has been paid to understanding the balance between two disparate forces on platform evolution. First, there are the internal interactions occurring between elements within the overall system, so-called "autogenic" factors. Into this category are the myriad of interactions between the reef-building organisms, or between those organisms and their physical or chemical environment. Second, are the "allogenic" forcings imposed by factors external to the system, such as sea-level oscillation. A slew of recent studies emphasize that autogenic forces can be as important as allogenic ones in sculpting the architecture of carbonate platforms (Purkis and Kohler, 2008; Purkis et al., 2015a, 2015b; Budd et al., 2016; Burgess, 2001, 2006; Burgess, 2016; Purkis et al., 2016b; Rankey, 2021). This study contributes to this overall body of work as again highlights that sea-level change is a poor predictor of the behavior of atoll islands in the Chagos and beyond.

6. Conclusions

By compiling data describing the dynamics of atoll-island coastlines for 20 islands in Peros Banhos Atoll and for the single island atop Diego Garcia Atoll, this paper has emphasized that whether impacted by humans, or not, these islands display multi-decadal stability, if island area is the considered metric. However, if the movement of the coastlines of these islands through time is considered, they are seen to be highly dynamic, with coastlines facing prevailing wave energy eroding and those situated in leeward positions extending. Human intervention is seen to amplify these dynamics in Diego Garcia. Of these two metrics of change, it is dynamic coastlines which are likely the major determinant as to whether an atoll island is suitable for long-term human habitation. Radical shifts in coastline position on sub-decadal timescales will frustrate the installation and maintenance of critical infrastructure, such as roads and utilities, exacerbate flooding, and challenge community resilience to climate change. At global scale, by assembling data from the literature, it is seen that the considered islands in the Chagos Archipelago display behavior consistent with those situated in the adjacent Maldives Archipelago, in that small islands tend to have more dynamic coastlines than large ones, a pattern also mirrored in the Pacific Ocean. No correlation is observed between the dynamics of 28 atolls distributed through the Indian and Pacific Oceans and rate of sea-level rise, suggesting local factors to be more important drivers of island dynamics than the fluctuation of eustatic sea level, at least on the decadal timescales considered by this study. It is hoped that these data will inform on the persistence and habitability of atoll islands in the face of climate change.

Supplementary data to this article can be found online at https://doi.org/10.1016/j.gloplacha.2021.103519.

Declaration of Competing Interest

The authors have no conflict of interest to declare and pledge that the submitted work is original.

References

Andréfouët, S., Bionaz, O., 2021. Lessons from a global remote sensing mapping project. A review of the impact of the Millennium Coral Reef Mapping Project for science and management. Sci. Total Environ. 145987.

Andréfouët, S., Muller-Karger, F.E., Robinson, J.A., Kranenburg, C.J., Torres-Pulliza, D., Spraggins, S.A., Murch, B., 2006. Global assessment of modern coral reef extent and diversity for regional science and management applications: a view from space. Jpn. Coral Reef Soc. Okinawa 2, 1732–1745.

Andréfouët, S., Guillaume, M.M.M., Delval, A., Rasoamanendrika, F.M.A., Blanchot, J., Bruggemann, J.H., 2013. Fifty years of changes in reef flat habitats of the Grand Récif of Toliara (SW Madagascar) and the impact of gleaning. Coral Reefs 32, 757–768.

Aslam, M., Kench, P.S., 2017. Reef island dynamics and mechanisms of change in Huvadhoo Atoll, Republic of Maldives, Indian Ocean. Anthropocene 18, 57–68.

Bailey, R.T., 2015. Quantifying transient post-overwash aquifer recovery for atoll islands in the Western Pacific. Hydrol. Process. 29, 4470–4482.

Barkey, B.L., Bailey, R.T., 2017. Estimating the impact of drought on groundwater resources of the Marshall Islands. Water 9, 41.

Beetham, E., Kench, P.S., Popinet, S., 2017. Future reef growth can mitigate physical impacts of sea-level rise on atoll islands. Earth's Future 5, 1002–1014.

Biribo, N., Woodroffe, C.D., 2013. Historical area and shoreline change of reef islands around Tarawa Atoll, Kiribati. Sustain. Sci. 8, 345–362.

Boberg, J., 2009. Litter Decomposing Fungi in Boreal forEsts. PhD Thesis. Swedish university of Agricultural Sciences, Uppsala, Sweden. https://pub.epsilon.slu.se/2136/ (accessed 10 December 2019).

Budd, D.A., Hajek, E.A., Purkis, S.J., 2016. Introduction to autogenic dynamics and self-organization in sedimentary systems. SEPM Spec. Publi. 106, 1–4.

Burgess, P.M., 2001. Modeling carbonate sequence development without relative sea-level oscillations. Geology 29, 1127–1130.

Burgess, P.M., 2006. The signal and the noise: forward modeling of allocyclic and autocyclic processes influencing peritidal carbonate stacking patterns. J. Sediment. Res. 76, 962–977.

Burgess, P.M., 2016. The future of the sequence stratigraphy paradigm: dealing with a variable third dimension. Geology 44, 335–336.

Chollett, I., Mumby, P.J., 2012. Predicting the distribution of *Montastraea* reefs using wave exposure. Coral Reefs 31, 493–503.

Church, J.A., White, N.J., Hunter, J.R., 2006. Sea-level rise at tropical Pacific and Indian Ocean islands. Glob. Planet. Chang. 53, 155–168.

Coleman, D.C., Callaham Jr., M.A., Crossley Jr., D.A., 2017. Fundamentals of Soil Ecology, third ed. Academic Press, London.

Collen, J.D., Garton, D.W., Gardner, J.P.A., 2009. Shoreline changes and sediment redistribution at Palmyra atoll (equatorial Pacific Ocean): 1874–present. J. Coast. Res. 25, 711–722.

Dickinson, W.R., 1999. Holocene Sea-level record on Funafuti and potential impact of global warming on Central Pacific atolls. Quat. Res. 51, 124–132.

Droxler, A.W., Jorry, S.J., 2021. The origin of modern atolls: challenging Darwin's deeply ingrained theory. Annu. Rev. Mar. Sci. 13, 537–573.

Dunne, R.P., Barbosa, S.M., Woodworth, P.L., 2012. Contemporary Sea level in the Chagos Archipelago, Central Indian Ocean. Glob. Planet. Chang. 82, 25–37.

Duvat, V.K., 2019. A global assessment of atoll island planform changes over the past decades. -level rise? WIREs Clim. Chang. 10, 557.

Duvat, V.K., 2020. Human-driven atoll island expansion in the Maldives. Anthropocene 32, 100265.

Duvat, V.K., Pillet, V., 2017. Shoreline changes in reef islands of the Central Pacific: Takapoto Atoll, Northern Tuamotu, French Polynesia. Geomorphology 282, 96–118.

Duvat, V.K., Salvat, B., Salmon, C., 2017. Drivers of shoreline change in atoll reef islands of the Tuamotu Archipelago, French Polynesia. Glob. Planet. Chang. 158, 134–154.

Eisenhauer, A., Heiss, G.A., Sheppard, C.R.C., Dullo, W.C., 1999. Reef and island formation and late Holocene Sea-level changes in the Chagos islands. Ecol. Chagos Archipelago 21–31.

Falkland, T., White, I., 2020. Freshwater availability under climate change. In: Kumar, L. (Ed.), Clim. Chang. Impacts in the Pacific. Springer Climate. Springer, Cham, pp. 403–448.

Flowers, T.J., Colmer, T.D., 2015. Plant Salt Tolerance: Adaptations in Halophytes. Ann. Bot. 115, 327–331.

Ford, M., 2012. Shoreline changes on an urban atoll in the Central Pacific Ocean: Majuro Atoll, Marshall Islands. J. Coast. Res. 28, 11–22.

Ford, M., 2013. Shoreline changes interpreted from multi-temporal aerial photographs and high-resolution satellite images: Wotje Atoll, Marshall Islands. Remote Sens. Environ. 135, 130–140.

Ford, M.R., Kench, P.S., 2014. Formation and adjustment of typhoon-impacted reef islands interpreted from remote imagery: Nadikdik atoll, Marshall Islands. Geomorphology 214, 216–222.

Ford, M.R., Kench, P.S., 2015. Multi-decadal shoreline changes in response to sea level rise in the Marshall Islands. Anthropocene 11, 14–24.

Ford, M.R., Kench, P.S., 2016. Spatiotemporal variability of typhoon impacts and relaxation intervals on Jaluit Atoll, Marshall Islands. Geology 44 (2), 159–162.

Graham, N.A.J., Purkis, S.J., Harris, A., 2009. Diurnal, land-based predation on shore crabs by moray eels in the Chagos Archipelago. Coral Reefs 28 (2) (397–397).

Graham, N.A., Wilson, S.K., Carr, P., Hoey, A.S., Jennings, S., MacNeil, M.A., 2018. Seabirds enhance coral reef productivity and functioning in the absence of invasive rats. Nature 559, 250–253.

Hamylton, S., East, H., 2012. A geospatial appraisal of ecological and geomorphic change on Diego Garcia Atoll, Chagos islands (British Indian Ocean Territory). Remote Sens. 4, 3444–3461.

Holdaway, A., Ford, M., Owen, S., 2021. Global-scale changes in the area of atoll islands during the 21st century. Anthropocene 33, 100282.

Hubbard, D., Gischler, E., Davies, P., Montaggioni, L., Camoin, G., Dullo, W.-C., Storlazzi, C., Field, M., Fletcher, C., Grossman, E., Sheppard, C., Lescinsky, H., Fenner, D., McManus, J., Scheffers, S., 2014. Island outlook: warm and swampy. Sci. 345, 1461.

Januchowski-Hartley, F.A., Graham, N.A., Wilson, S.K., Jennings, S., Perry, C.T., 2017. Drivers and predictions of coral reef carbonate budget trajectories. Proc. R. Soc. B Biol. Sci. 284 (1847) (20162533).

Kaluwin, C., Smith, A., 1997. Coastal vulnerability and integrated coastal zone management in the South Pacific Island region. J. Coast. Res. 24, 95–106.

Kench, P.S., Brander, R.W., 2006. Response of reef island shorelines to seasonal climate oscillations: south Maalhosmadulu atoll, Maldives. J. Geophys. Res. Earth Surf. 111.

Kench, P.S., McLean, R.F., Nichol, S.N., 2005. Newmodel of reef-island evolution: Maldives, Indian Ocean. Geology 33, 145–148.

Kench, P.S., Thompson, D., Ford, M.R., Ogawa, H., McLean, R.F., 2015. Coral islands defy sea-level rise over the past century: records from a Central Pacific Atoll. Geology 43, 515–518.

Kench, P.S., Ford, M.R., Owen, S.D., 2018. Patterns of island change and persistence offer alternate adaptation pathways for atoll nations. Nat. Commun. 9, 1–7.

Le Cozannet, G., Garcin, M., Petitjean, L., Cazenave, A., Becker, M., Meyssignac, B., Walker, P., Devilliers, C., Le Brun, O., Lecacheux, S., Baills, A., 2013. Exploring the relation between sea level rise and shoreline erosion using sea level reconstructions: an example in French Polynesia. J. Coast. Res. 65, 2137–2142.

Masselink, G., Pattiaratchi, C.B., 2001. Seasonal changes in beach morphology along the sheltered coastline of Perth, Western Australia. Mar. Geol. 172, 243–263.

McGowan, A., Broderick, A.C., Godley, B.J., 2008. Seabird populations of the Chagos Archipelago: an evaluation of Important Bird Area sites. Oryx. 42, 424–429.

McLean, R., Kench, P., 2015. Destruction or persistence of coral atoll islands in the face of 20th and 21st century sea-level rise? WIREs Clim. Chang. 6, 445–463.

Merrifield, M., Aarup, T., Allen, A., Aman, A., Caldwell, P., Bradshaw, E., Fernandes, R. M.S., Hayashibara, H., Hernandez, F., Kilonsky, B., Martin Miguez, B., 2009. The glob. sea level observing syst. (GLOSS). Proc. Ocean Obs. 9.

Morgan, K.M., Kench, P.S., 2016. Parrotfish erosion underpins reef growth, sand talus development and island building in the Maldives. Sediment. Geol. 341, 50–57.

Newnham, T.J., Browne, N.K., Bumbak, J., Loudon, L., Wellington, H., Shedrawi, G., Hacker, J., O'Leary, M., 2020. Long-term (70-year) monitoring of reef structure through high-resolution multidecadal aerial imagery. Coral Reefs 39, 1859–1870.

Nicholls, R.J., Cazenave, A., 2010. Sea-level rise and its impact on coastal zones. Sci. 328, 1517–1520.

Perry, C.T., Morgan, K.M., 2017. Bleaching drives collapse in reef carbonate budgets and reef growth potential on southern Maldives reefs. Sci. Rep. 7, 40581.

Perry, C.T., Kench, P.S., Smithers, S.G., Riegl, B., Yamano, H., O'Leary, M.J., 2011. Implications of reef ecosystem change for the stability and maintenance of coral reef islands. Glob. Chang. Biol. 17, 3679–3696.

Perry, C.T., Kench, P.S., Smithers, S.G., Yamano, H., O'Leary, M., Gulliver, P., 2013. Time scales and modes of reef lagoon infilling in the Maldives and controls on the onset of reef island formation. Geology 41, 1111–1114.

Perry, C.T., Kench, P.S., O'Leary, M.J., Morgan, K.M., Januchowski-Hartley, F., 2015. Linking reef ecology to island building: parrotfish identified as major producers of island- building sediment in the Maldives. Geology 43, 503–506.

Perry, C.T., Alvarez-Filip, L., Graham, N.A., Mumby, P.J., Wilson, S.K., Kench, P.S., Manzello, D.P., Morgan, K.M., Slangen, A.B., Thomson, D.P., Januchowski-Hartley, F., 2018. Loss of coral reef growth capacity to track future increases in sea level. Nature 558, 396–400.

Purkis, S.J., Klemas, V.V., 2011. Remote Sensing and Global Environmental Change. Wiley-Blackwell, Oxford, U.K, p. 367.

Purkis, S.J., Kohler, K.E., 2008. The role of topography in promoting fractal patchiness in a carbonate shelf landscape. Coral Reefs 27, 977–989.

Purkis, S.J., Kohler, K.E., Riegl, B.M., Rohmann, S.O., 2007. The statistics of natural shapes in modern coral reef landscapes. J. Geol. 115, 493–508.

Purkis, S.J., Graham, N.A.J., Riegl, B.M., 2008. Predictability of Reef fish Diversity and Abundance using Remote Sensing Data in Diego Garcia (Chagos Archipelago). Coral Reefs 27, 167–178.

Purkis, S.J., Casini, G., Hunt, D., Colpaert, A., 2015a. Morphometric patterns in Modern carbonate platforms can be applied to the ancient rock record: Similarities between Modern Alacranes Reef and Upper Palaeozoic platforms of the Barents Sea. Sediment. Geol. 321, 49–69.

Purkis, S.J., Rowlands, G.P., Kerr, J.M., 2015b. Unravelling the influence of water depth and wave energy on the facies diversity of shelf carbonates. Sedimentology 62, 541–565.

Purkis, S.J., Gardiner, R., Johnston, M.W., Sheppard, C.R., 2016a. A half-century of coastline change in Diego Garcia–the largest atoll island in the Chagos. Geomorphology 261, 282–298.

Purkis, S.J., Vd Koppel, J., Burgess, P.M., 2016b. Spatial self-organization in carbonate depositional environments. pp. 53-66. In: Budd, D.A., Hajek, E.A., Purkis, S.J. (Eds.), 2016. Autogenic Dynamics and Self-Organization in Sediment. Systems, Spec. Publi. 106: SEPM (Society for Sedimentary Geology), Tulsa, Oklahoma (216 p).

Purkis, S.J., Gleason, A.C., Purkis, C.R., Dempsey, A.C., Renaud, P.G., Faisal, M., Saul, S., Kerr, J.M., 2019. High-resolution habitat and bathymetry maps for 65,000 sq. km of Earth's remotest coral reefs. Coral Reefs 38, 467–488.

Quataert, E., Storlazzi, C., Van Rooijen, A., Cheriton, O., Van Dongeren, A., 2015. The influence of coral reefs and climate change on wave-driven flooding of tropical coastlines. Geophys. Res. Lett. 42, 6407–6415.

Rankey, E.C., 2011. Nature and stability of atoll island shorelines: Gilbert Island chain, Kiribati, equatorial Pacific. Sedimentology 58, 1831–1859.

Rankey, E.C., 2021. Platform-top reef sand apron morphodynamics and the half-empty bucket. Sediment. Geol. 412, 105825.

Richmond, R.H., 1993. Coral reefs: present problems and future concerns resulting from anthropogenic disturbance. Am. Zool. 33, 524–536.

Roy, P., Connell, J., 1991. Climatic change and the future of atoll states. J. Coast. Res. 1057-1075.

Ryan, E.J., Hanmer, K., Kench, P.S., 2019. Massive corals maintain a positive carbonate budget of a Maldivian upper reef platform despite major bleaching event. Sci. Rep. 9 (1), 1–11.

Schlager, W., 1993. Accommodation and supply—a dual control on stratigraphic sequences. Sediment. Geol. 86, 111–136.

Sheehan, E.V., Hosegood, P., Game, C.A., Attrill, M.J., Tickler, D., Wootton, M., Johns, D. G., Meeuwig, J.J., 2019. The effect of deep oceanic flushing on water properties and ecosystem functioning within atolls in the British Indian Ocean Territory. Front. Mar. Sci. 6, 512.

Sheppard, C.R., 1981. The groove and spur structures of Chagos atolls and their coral zonation. Estuar. Coast. Shelf Sci. 12 (5), 549–IN2.

Sheppard, C.R., 2007. Effects of the tsunami in the Chagos Archipelago. Atoll Res. Bull. 544, 135–148.

Sheppard, C.R., 2016. Changes to the Natural history of Islands in the Chagos Atolls, Central Indian Ocean, during Human Settlement (1780–1969), and prospects for Restoration. Atoll Res. Bull. 29, 612.

Sheppard, C., Dixon, D.J., Gourlay, M., Sheppard, A., Payet, R., 2005. Coral mortality increases wave energy reaching shores protected by reef flats: examples from the Seychelles. Estuar. Coast. Shelf Sci. 64, 223–234.

Sheppard, C.R., Ateweberhan, M., Bowen, B.W., Carr, P., Chen, C.A., Clubbe, C., Craig, M.T., Ebinghaus, R., Eble, J., Fitzsimmons, N., Gaither, M.R., 2012. Reefs and islands of the Chagos Archipelago, Indian Ocean: why it is the world's largest no-take marine protected area. Aquat. Conserv. Mar. Freshw. Ecosyst. 22, 232–261.

Sheppard, C., Sheppard, A., Mogg, A., Bayley, D., Dempsey, A.C., Roache, R., Turner, J., Purkis, S., 2017. Coral bleaching and mortality in the Chagos Archipelago. Atoll Res. Bull. 613, 1–26.

Sheppard, C., Sheppard, A., Fenner, D., 2020. Coral mass mortalities in the Chagos Archipelago over 40 years: Regional species and assemblage extinctions and indications of positive feedbacks. Mar. Pollut. Bull. 154, 111075.

Stoddart, D.R., 1971. Terrestrial fauna of Diego Garcia and other Chagos atolls. Atoll Res. Bull. 149, 163–170.

Storlazzi, C.D., Elias, E.P.L., Berkowitz, P., 2015. Many atolls may be uninhabitable within decades due to climate change. Sci. Rep. 5, 14546.

Taylor, K.H., Purkis, S.J., 2012. Evidence for the southward migration of mud banks in Florida Bay. Mar. Geol. 311–314, 52–56.

Tuck, M.E., Kench, P.S., Ford, M.R., Masselink, G., 2019. Physical modelling of the response of reef islands to sea-level rise. Geology 47, 803–806.

Van Woesik, R., Cacciapaglia, C.W., 2018. Keeping up with sea-level rise: Carbonate production rates in Palau and Yap, western Pacific Ocean. PLoS One 13, e0197077.

Webb, A.P., Kench, P.S., 2010. The dynamic response of reef islands to sea-level rise: evidence from multi-decadal analysis of island change in the Central Pacific. Glob. Planet. Chang. 72, 234–246.

Woodroffe, C.D., 2005. Late quaternary Sea-level highstands in the central and Eastern Indian Ocean: a review. Glob. Planet. Chang. 49, 121–138.

Woodroffe, C.D., 2008. Reef-island topography and the vulnerability of atolls to sea-level rise. Glob. Planet. Chang. 62, 77–96.

Yates, M.L., Le Cozannet, G., Garcin, M., Salaï, E., Walker, P., 2013. Multidecadal atoll shoreline change on Manihi and Manuae, French Polynesia. J. Coast. Res. 29, 870–882.